Letter

General scattering and electronic states in a quantum-wire network of moiré systems

Chen-Hsuan Hsu [1,2,3] Daniel Loss,[3,4] and Jelena Klinovaja [4]

[1] *Yukawa Institute for Theoretical Physics, Kyoto University, Kyoto 606-8502, Japan*
[2] *Institute of Physics, Academia Sinica, Taipei 115, Taiwan*
[3] *RIKEN Center for Emergent Matter Science, Wako, Saitama 351-0198, Japan*
[4] *Department of Physics, University of Basel, Klingelbergstrasse 82, CH-4056 Basel, Switzerland*

(Received 21 February 2023; revised 1 September 2023; accepted 5 September 2023; published 21 September 2023)

We investigate electronic states in a two-dimensional network consisting of interacting quantum wires, a model adopted for twisted bilayer systems. We construct general operators which describe various scattering processes in the system. In a twisted bilayer structure, the moiré periodicity allows for generalized umklapp scatterings, leading to a class of correlated states at certain fractional fillings. We identify scattering processes which can lead to an insulating gapped bulk with gapless chiral edge modes at fractional fillings, resembling the quantum anomalous Hall effect recently observed in twisted bilayer graphene. Finally, we demonstrate that the description can be useful in predicting spectroscopic and transport features to detect and characterize the chiral edge modes in the moiré-induced correlated states.

DOI: 10.1103/PhysRevB.108.L121409

Moiré bilayer structures provide a platform for strongly correlated systems, where unconventional states of matter emerge [1–4] as a consequence of flat energy bands [5]. Since the discovery of correlated insulating states and superconductivity in twisted bilayer graphene (TBG) [6,7], various exotic states or features have been observed [8], including nematicity [9–12], pressure-enhanced superconductivity [13], strange metal [14,15], cascade of transitions [16,17], orbital magnetism [18,19], independent superconducting and correlated insulating states [20–22], fragile correlated states against twist angle disorder [23], entropy-driven phase transition [24,25], unconventional superconductivity [26], and spin-orbit-driven ferromagnetism [27].

In addition to features that resemble existing strongly correlated systems such as cuprates and iron-based superconductors, there are observations suggesting the existence of topological phases. Specifically, nonlocal transport demonstrated the presence of chiral edge modes at $3/4$ filling in TBG [28], accompanied by the quantization of Hall resistance at zero magnetic fields [29]. More recent studies revealed a series of quantum anomalous Hall or Chern insulators with Chern numbers $C = \pm 1, \pm 2$, and ± 3 at $\pm 3/4, \pm 1/2$, and $\pm 1/4$ fillings, respectively [30–32]. Furthermore, there is experimental indication of a many-body origin for the topological phases [27,30–36]. The observations on various electronic states motivated theoretical studies on TBG [37–53] and the development of moiré electronics, including structures beyond bilayers [54–63] and materials other than graphene [64–69].

A major theoretical challenge in strongly correlated moiré systems involves incorporating many-body effects with numerous atoms due to the large moiré unit cell. It is thus crucial to identify the relevant degrees of freedom to construct an effective model for efficient quantitative analysis. Remarkably, correlated phenomena in TBG can be investigated in the context of (Tomonaga-)Luttinger liquids, which inherently includes electron-electron interactions [70–72]. Specifically, in the presence of an interlayer potential difference, one-dimensional channels emerge at domain walls between AB- and BA-stacking regions [73–75] and form a triangular quantum-wire network illustrated in Fig. 1; we also note spectroscopic [9–11,76,77] and transport [78] features of the domain-wall network [79]. These findings motivated theoretical studies on network models based on Luttinger liquids [80–84], reminiscent of earlier works on (crossed) sliding Luttinger liquids proposed for cuprates [85–88] and

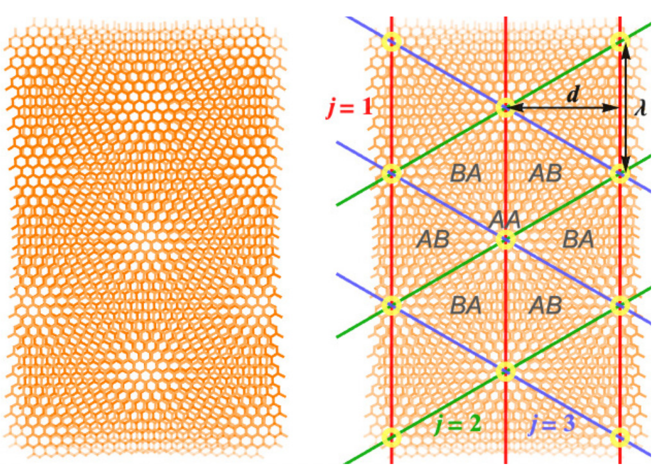

FIG. 1. Moiré pattern and quantum-wire network of the TBG. When two graphene monolayers (orange) are stacked with a misalignment, there appears a moiré pattern with the wavelength $\lambda = a_0/[2\sin(\theta/2)]$, monolayer lattice constant a_0, and the angle θ between the layers. The moiré pattern results in three sets of parallel quantum wires, plotted in distinct colors and labeled by j, with the interwire distance $d = \sqrt{3}\lambda/2$.

the coupled-wire constructions of various quantum Hall states [89–99]. From a different perspective, moiré systems provide mesoscopic realizations of coupled-wire systems originally proposed for entirely distinct systems [85–88].

In this work, we extend the network models [80–84] to explore the possibility of topological phases in moiré systems. We construct operators describing general scattering processes based on conservation laws and investigate the resulting electronic states. In moiré structures, the periodic potential allows for generalized umklapp scatterings, which lead to correlated states at fractional fillings. Remarkably, we identify processes that lead to a gapped bulk with gapless modes along the edges, resembling the observed Chern insulators in TBG [28–35]. Furthermore, we demonstrate that this description can be useful by making concrete predictions for spectroscopic and transport features. In addition to TBG, our mechanism can apply to other nanoscale systems forming arrays of one-dimensional channels, such as twisted moiré bilayers formed by WTe_2 [100] or topological insulators [101,102], as well as strain-engineered graphene [103].

Bosonization. We introduce the fermion field $\psi^{(j)}_{\ell m\sigma}$ with the array index $j \in \{1, 2, 3\}$, wire index $m \in [1, N_\perp]$ within each array, the index $\ell \in \{R \equiv +, L \equiv -\}$ labeling the moving direction, and spin $\sigma \in \{\uparrow \equiv +, \downarrow \equiv -\}$; see Fig. 2. The fermion field can be bosonized as

$$\psi^{(j)}_{\ell m\sigma}(x) = \frac{U^j_{\ell m\sigma}}{\sqrt{2\pi a}} e^{i\ell k_F x} \times e^{\frac{-i}{\sqrt{2}}\left[\ell\phi^j_{cm}(x) - \theta^j_{cm}(x) + \ell\sigma\phi^j_{sm}(x) - \sigma\theta^j_{sm}(x)\right]}, \tag{1}$$

with the Klein factor $U^j_{\ell m\sigma}$, short-distance cutoff a, local coordinate x, Fermi wave vector k_F (identical for all wires), and the index $\xi \in \{c \equiv +, s \equiv -\}$ for the charge/spin sector of the boson fields $\phi^j_{\xi m}$ and $\theta^j_{\xi m}$, satisfying

$$\left[\phi^j_{\xi m}(x), \theta^{j'}_{\xi' m'}(x')\right] = i\frac{\pi}{2}\mathrm{sgn}(x' - x)\delta_{jj'}\delta_{\xi\xi'}\delta_{mm'}. \tag{2}$$

Below we omit the Klein factor and x whenever possible.

The unperturbed Hamiltonian $H_0 + H_{\mathrm{fs}}$ describes a crossed sliding Luttinger liquid at the fixed point [82], with the kinetic energy H_0 and marginally relevant forward scattering terms H_{fs} quadratic in the density operator $\propto \partial_x \phi^j_{cm}$. In addition, there exist intrawire or interwire backscattering processes, arising from electron-electron interactions and/or tunnelings, which can destabilize the fixed point characterized by the quadratic terms, as those in coupled-wire systems [89–99]. Since the bandwidth W serves as high-energy cutoff [104], the dimensionless coupling g/W, with the strength g characterizing a general scattering, takes a larger value in (quasi-)flat-band systems, allowing for higher-order scatterings to play a more significant role. As in Refs. [89,95], we do not specify H_{fs}; for demonstration, a specific model [82,85–88] is presented in the Supplemental Material (SM) [105]. Below we construct operators describing general scatterings, including higher-order processes (previously discussed in multiband wires [106,107]), and discuss the resulting electronic states.

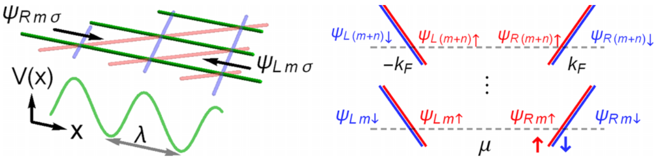

FIG. 2. Quantum-wire network in a moiré structure. Left: For each wire, we define the local coordinate x and fermion fields $\psi_{\ell m\sigma}$, which experience a periodic potential $V(x)$ generated by the moiré structure. Right: Each array consists of parallel wires with the chemical potential μ and Fermi wave vector k_F, where we linearize the energy dispersion and bosonize the fields with Eq. (1).

General scattering operator. We consider the operator

$$O_{\left\{s^j_{\ell p\sigma}\right\}} = \sum_{m=1}^{N_\perp}\prod_{p=0}\prod_{j=1}^{3}\left[\psi^{(j)}_{R(m+p)\uparrow}\right]^{s^j_{Rp\uparrow}}\left[\psi^{(j)}_{L(m+p)\uparrow}\right]^{s^j_{Lp\uparrow}} \times \left[\psi^{(j)}_{R(m+p)\downarrow}\right]^{s^j_{Rp\downarrow}}\left[\psi^{(j)}_{L(m+p)\downarrow}\right]^{s^j_{Lp\downarrow}}, \tag{3}$$

where the subscript $\{s^j_{\ell p\sigma}\}$ denotes an integer set for all values of (j, ℓ, p, σ) with $p \in$ integers. The set characterizes O; a negative value implies Hermitian conjugate: $\psi^s \equiv (\psi^\dagger)^{|s|}$ for $s < 0$. A nonzero s for a given p indicates that the pth nearest neighbor wires participate in the scattering. While O can in principle involve any number of wires, physically one expects s to vanish for large p in systems subject to finite-range interactions.

The operator O describes scatterings within an array when s is nonzero for a single j value. The corresponding renormalization-group (RG) relevance condition is given by $\Delta_{s^j_{\ell p\sigma}} < 2$, where the scaling dimension $\Delta_{s^j_{\ell p\sigma}}$ is determined by $H_0 + H_{\mathrm{fs}}$. In a network consisting of crossed wires, interarray scatterings can occur at wire intersections [81,82,87,88], as characterized by Eq. (3) with nonzero s for multiple j values. References [81,82] showed that such scatterings can induce superconducting and insulating phases in moiré bilayers. However, the RG relevance condition in this case is more stringent: $\Delta_{s^j_{\ell p\sigma}} < 1$, since the corresponding operator enters the effective action without involving the spatial integral [105]. Furthermore, the interarray scatterings are independent of the filling factor. To explore correlated states from more RG relevant scatterings, below we examine scatterings within an array and suppress j.

We start with the constraints on possible $s_{\ell p\sigma}$ values. In the absence of proximity-induced "external" pairing, the global particle number or charge is conserved, giving

$$\sum_{p,\sigma}(s_{Rp\sigma} + s_{Lp\sigma}) = 0. \tag{4}$$

For clean systems, the momentum conservation gives additional constraint. Here, the moiré structure plays an important role, as it creates a periodic potential, which partially relaxes the constraint from the momentum conservation. As illustrated in Fig. 2, electrons experience a moiré potential with a spatial period of λ. This leads to a generalized condition for momentum conservation,

$$k_F\sum_{p,\sigma}(s_{Rp\sigma} - s_{Lp\sigma}) = \frac{2\pi}{\lambda} \times \text{integer}, \tag{5}$$

which allows us to organize $O_{\{s_{\ell p\sigma}\}}$ into two categories.

In the first category, scatterings are allowed for any k_F independent of the filling factor, provided that the coefficients satisfy

$$\sum_{p,\sigma}(s_{Rp\sigma} - s_{Lp\sigma}) = 0. \tag{6}$$

Together with the constraint in Eq. (4), we get

$$\sum_{p,\sigma} s_{Rp\sigma} = \sum_{p,\sigma} s_{Lp\sigma} = 0, \tag{7}$$

meaning that the numbers of the left- and right-moving particles are individually conserved. We refer to these processes as *conventional scatterings*, which characterize electronic states corresponding the "crystalline states" in Ref. [89].

At certain fillings, on the other hand, another category of scatterings can take place even when Eq. (6) is not fulfilled. The momentum difference due to the number imbalance between the left- and right-moving particles can be compensated by the "crystal momentum" proportional to the reciprocal lattice vector $2\pi/\lambda$. With Eqs. (4)–(5) and the relation between the filling factor and Fermi wave vector $\nu = k_F\lambda/\pi$ [104], we get a condition on the filling factor,

$$\nu = \frac{P}{\sum_{p,\sigma} s_{Rp\sigma}}, \tag{8}$$

with a nonzero integer P. In our description, $\nu = 1$ corresponds to 4 electrons per moiré unit cell in TBG [81,82]. Since these processes are feasible owing to the presence of the moiré periodic potential, in analogy to Refs. [104,108], we refer to the second category as *moiré umklapp scatterings* and the corresponding states of matter *moiré correlated states*.

For both categories, the bosonization in Eq. (1) gives

$$O_{\{s_{\ell p\sigma}\}} = \sum_{m=1} \exp\left\{\frac{i}{\sqrt{2}}\sum_p [S_{p,c}\phi_{c(m+p)} + \bar{S}_{p,c}\theta_{c(m+p)} + S_{p,s}\phi_{s(m+p)} + \bar{S}_{p,s}\theta_{s(m+p)}]\right\}, \tag{9}$$

with the coefficients

$$S_{p,\xi} = s_{Lp\uparrow} - s_{Rp\uparrow} + \xi(s_{Lp\downarrow} - s_{Rp\downarrow}), \tag{10a}$$

$$\bar{S}_{p,\xi} = s_{Lp\uparrow} + s_{Rp\uparrow} + \xi(s_{Lp\downarrow} + s_{Rp\downarrow}). \tag{10b}$$

The global charge conservation requires $\sum_p \bar{S}_{p,c} = 0$. The momentum conservation requires $\sum_p S_{p,c} = 0$ for conventional scatterings and $\nu \sum_p S_{p,c} = 2P$ for moiré umklapp scatterings. If the charge (spin) is conserved for a fixed p, the coefficient $\bar{S}_{p,c}$ ($\bar{S}_{p,s}$) vanishes. While there is in general no constraint on $\bar{S}_{p,s}$, for simplicity we choose $\bar{S}_{p,s} = 0$, as operators with nonzero $\bar{S}_{p,s}$ are typically less RG relevant.

The conventional scatterings fulfilling Eq. (7) include charge-density-wave couplings, Josephson couplings, and hoppings. They lead to charge density wave, superconducting, and Fermi liquid states, respectively [105]. In addition, the twisted structure enables moiré umklapp scatterings, which we discuss below.

Moiré correlated states. The moiré umklapp scatterings can be further categorized into four types, depending on whether they involve multiple wires, whether they involve scatterings between wires, and whether they conserve the particle number for each wire. While the operator in Eq. (3) describes general processes at fractional fillings in Eq. (8), below we provide specific examples allowed at $\nu = P/4$.

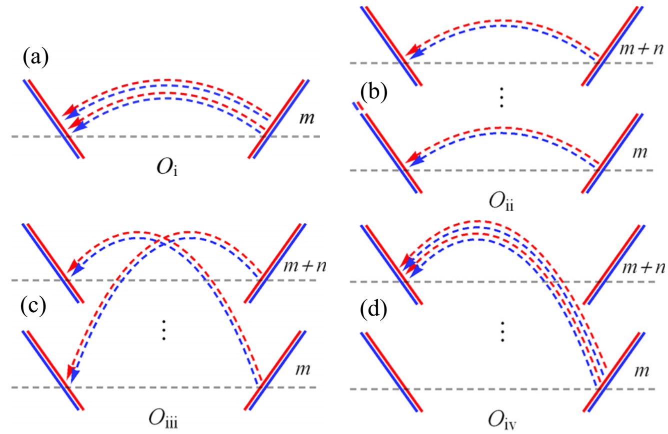

FIG. 3. Examples for moiré umklapp scatterings at $\nu = P/4$. (a) O_{i}, characterized by Eq. (3) with $(s_{R0\sigma}, s_{L0\sigma}) = (2, -2)$. (b) O_{ii}, with $(s_{R0\sigma}, s_{L0\sigma}, s_{Rn\sigma}, s_{Ln\sigma}) = (1, -1, 1, -1)$. (c) O_{iii}, with $(s_{R0\sigma}, s_{L0\sigma}, s_{Rn\sigma}, s_{Ln\sigma}) = (1, -1, 1, -1)$. (d) O_{iv}, with $(s_{R0\sigma}, s_{L0\sigma}, s_{Rn\sigma}, s_{Ln\sigma}) = (2, 0, 0, -2)$. Here we illustrate processes that are invariant upon changing the spin sign; see Table S1 for more general cases [105].

We start with processes involving only single wires and denote the corresponding operator as O_{i}. In Fig. 3(a), we illustrate the process with nonzero coefficients, $(s_{R0\sigma}, s_{L0\sigma}) = (2, -2)$ for both $\sigma = \uparrow$ and $\sigma = \downarrow$. The example describes a process where four electrons at k_F are backscattered to $-k_F$, with the total momentum difference $8k_F = 4\nu \times (2\pi/\lambda)$ compensated by the moiré potential. Next, there are umklapp processes involving multiple wires with correlated intrawire scatterings, labeled as O_{ii}. The simplest case involves two nth nearest neighboring wires, with an example in Fig. 3(b); we note that the number of backscatterings in each wire can be different. Furthermore, we have O_{iii} involving interwire scatterings while still conserving the particle number for each wire. As mentioned above, the latter constraint implies $\bar{S}_{p,c} = 0$ for any p, as in the case for O_{i} and O_{ii}. For instance, in Fig. 3(c) we show a process involving two nth nearest neighbor wires. Finally, allowing for processes which do not conserve the particle number for some wires, we have O_{iv}, with $\bar{S}_{p,c} \neq 0$ for some p. In Fig. 3(d) we plot a two-wire process. In addition to the depicted examples, we present the moiré umklapp scatterings in Table S1 in the SM [105], covering a broader range of fillings and higher-order processes.

For O_{i}, O_{ii}, and O_{iii}, one can obtain a sum of sine-Gordon terms upon bosonization. Taking Fig. 3(a) as an example, we have $O_{\mathrm{i}} + O_{\mathrm{i}}^\dagger \propto \sum_m \cos(4\sqrt{2}\phi_{cm})$. When the corresponding operator is RG relevant, it gaps out all the ϕ_{cm} fields and leads to a correlated insulating state at fractional fillings. In the strong-coupling limit, ϕ_{cm} is pinned to a minimum of the cosine. A kink excitation corresponds to a tunneling process between two neighboring minima, where ϕ_{cm} changes its value by $\pm\pi/(2\sqrt{2})$. We find that the system hosts fractional excitations with charge $\pm e/2$ associated with the kink. In contrast to the first three types, the states resulting from O_{iv} can host gapless edge modes, which we demonstrate next.

Chiral edge modes. We consider O_{iv} scattering involving the nth nearest neighbor wires, which allows us to keep only a few nonzero coefficients in Eq. (10); i.e., $S_{n,c} = S_{0,c}$ and $\bar{S}_{n,c} = -\bar{S}_{0,c}$. To proceed, we introduce chiral fields $\Phi_{\ell m} = -\ell\phi_{cm} + f\theta_{cm}$ with $f = -\bar{S}_{0,c}/S_{0,c}$, which satisfy

$$[\Phi_{\ell m}(x), \Phi_{\ell' m'}(x')] = i\ell\pi\delta_{\ell\ell'}\delta_{mm'} f\,\text{sgn}(x - x'). \quad (11)$$

The transformation leads to

$$O_{\text{iv}} + O_{\text{iv}}^{\dagger} \propto \sum_{m=1} \cos\left\{\frac{S_{0,c}}{\sqrt{2}}[\Phi_{L(m+n)} - \Phi_{Rm}]\right\}. \quad (12)$$

The expression indicates the presence of n gapless chiral modes $\Phi_{L,1}, \ldots, \Phi_{L,n}$ at one edge and, similarly, n gapless right-moving modes at the opposite edge. To proceed, we define $\tilde{\Phi}_{m,n} = [\Phi_{L(m+n)} - \Phi_{Rm}]/2$ and get $O_{\text{iv}} + O_{\text{iv}}^{\dagger} \propto \sum_{m=1} \cos(\sqrt{2}S_{0,c}\tilde{\Phi}_{m,n})$. Using Eq. (11), it can be shown that the $\tilde{\Phi}_{m,n}$ fields for any m commute [105], gapping out the bulk modes in the interior of the system. Similar to the correlated states induced by O_{i}-O_{iii}, the system hosts fractional excitations, with charge $\pm 2e/S_{0,c}$. We expect formation of chirality domains, hosting gapless chiral modes at domain walls [105]. While the formation of domain walls costs energy, (disorder-induced) local magnetic moments can trigger their formation, which increases the entropy and therefore lowers the free energy at finite temperatures. Remarkably, a finite magnetic field is required to train domains in order to stabilize edge modes with a definite chirality in micrometer-size samples [28,29].

Using the Landauer-Büttiker formalism [109–112], we obtain quantized Hall resistance $h/(ne^2)$. For $n = 1$ and $\nu = 3/4$, it leads to a value of h/e^2, as observed in Ref. [29]. In consequence, the system exhibits quantum anomalous Hall effect with chiral edge modes and fractional excitations. We note that it is possible to reproduce a sequence of Chern insulating states with $C = \pm 1, \pm 2$, and ± 3 (corresponding to n here) at fillings $\nu = \pm 3/4, \pm 1/2$, and $\pm 1/4$, respectively. The complete sequence was observed in Refs. [30–32], while a partial set was reported in Refs. [27–29,33–36].

To demonstrate that O_{iv} can be RG relevant, we compute its scaling dimension and get [105]

$$\Delta_{\text{iv}} = \frac{1}{2}|S_{0,c}\bar{S}_{0,c}|\left(1 + \frac{2U}{\hbar v_0}\right)^{-\frac{1}{2}}, \quad (13)$$

with the $q \sim 0$ Fourier component U of the density-density interaction and the velocity v_0. In consequence, for a given scattering process, the RG relevance condition $\Delta_{\text{iv}} < 2$ is fulfilled for sufficiently large U.

Experimental signatures. The predicted chiral edge modes can be characterized by spectroscopic and transport measurements. For simplicity we consider a moiré correlated state hosting a single edge mode [105]. Utilizing scanning tunneling spectroscopy, one can probe the local density of states, which follows a universal scaling curve for energy ϵ and temperature T,

$$\rho(\epsilon) \propto T^{\frac{1}{f}-1} \cosh\left(\frac{\epsilon}{2k_{\text{B}}T}\right)\left|\Gamma\left(\frac{1}{2f} + i\frac{\epsilon}{2\pi k_{\text{B}}T}\right)\right|^2. \quad (14)$$

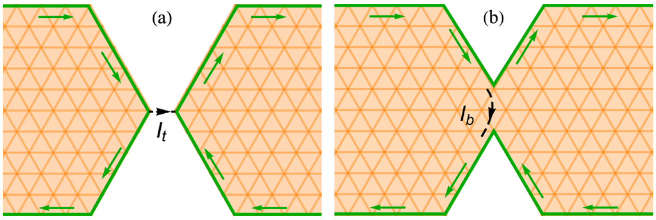

FIG. 4. QPC setups for systems in a moiré correlated state with a gapped bulk (orange) and gapless chiral edge modes (green). The setup (a) allows for tunnel current I_{t}. The setup (b) leads to backscattering current I_{b} and conductance correction δG.

In contrast to carbon nanotubes [113,114] or helical liquids [115,116], the scaling exponent here does not depend on H_{fs}, demonstrating the topological nature of the chiral edge modes.

Alternatively, one can probe the chiral edge modes via charge transport [117–122]. Specifically, we consider two setups employing quantum point contacts (QPCs). The setup in Fig. 4(a) allows for interedge tunneling with a current described by another universal scaling formula,

$$I_{\text{t}} \propto T^{\frac{2}{f}-1} \sinh\left(\frac{eV}{2k_{\text{B}}T}\right)\left|\Gamma\left(\frac{1}{f} + i\frac{eV}{2\pi k_{\text{B}}T}\right)\right|^2, \quad (15)$$

with bias voltage V. On the other hand, the interedge backscattering in Fig. 4(b) leads to power-law correction in the (differential) conductance with the magnitude $|\delta G| \propto \max(eV, k_{\text{B}}T)^{2f-2}$. Unlike fractional quantum Hall states [117–121], the scaling exponents depend on f here, but not directly on the filling factor ν. The same QPC geometry can be used to detect fractional charges through shot noise [123–125].

As a remark, while the theoretical works establishing a quantum-wire network in moiré bilayers [73,75] involve a sufficiently large interlayer potential difference, achievable via voltage gates, we expect that the network can form under broader conditions [9–11,76–78]. Namely, a spectral gap can be generally induced in graphene-based devices through coupling to other layered materials or substrates, depending on their stacking configurations [27–29,36,126–130]. Therefore, a gap with a spatially dependent sign can be achieved through nanoscale engineering [82,103,131], leading to a network of gapless domain walls that separate regions with opposing gap signs.

Finally, we point out that, through the proposed experimental verification, the system can reveal the long-sought intrinsic fractional quantum anomalous Hall states, where topology and many-body physics interplay. Upon inducing superconductivity (e.g., by proximity), moiré correlated states hosting fractional edge modes provide a platform to stabilize parafermion edge or zero modes [132–141] even without magnetic fields.

We thank Y.-Y. Chang, C.-H. Chung, and C.-T. Ke for interesting discussions. This work was financially supported by JSPS KAKENHI Grant No. 19H05610, the Swiss National Science Foundation (Switzerland), the NCCR QSIT, and the National Science and Technology Council (NSTC), Taiwan, through Grant No. NSTC-112-2112-M-001-025-MY3.

[1] E. Y. Andrei and A. H. MacDonald, Graphene bilayers with a twist, Nat. Mater. **19**, 1265 (2020).
[2] L. Balents, C. R. Dean, D. K. Efetov, and A. F. Young, Superconductivity and strong correlations in moiré flat bands, Nat. Phys. **16**, 725 (2020).
[3] E. Y. Andrei, D. K. Efetov, P. Jarillo-Herrero, A. H. MacDonald, K. F. Mak, T. Senthil, E. Tutuc, A. Yazdani, and A. F. Young, The marvels of moiré materials, Nat. Rev. Mater. **6**, 201 (2021).
[4] D. M. Kennes, M. Claassen, L. Xian, A. Georges, A. J. Millis, J. Hone, C. R. Dean, D. N. Basov, A. N. Pasupathy, and A. Rubio, Moiré heterostructures as a condensed-matter quantum simulator, Nat. Phys. **17**, 155 (2021).
[5] R. Bistritzer and A. H. MacDonald, Moiré bands in twisted double-layer graphene, Proc. Natl. Acad. Sci. USA **108**, 12233 (2011).
[6] Y. Cao, V. Fatemi, S. Fang, K. Watanabe, T. Taniguchi, E. Kaxiras, and P. Jarillo-Herrero, Unconventional superconductivity in magic-angle graphene superlattices, Nature (London) **556**, 43 (2018).
[7] Y. Cao, V. Fatemi, A. Demir, S. Fang, S. L. Tomarken, J. Y. Luo, J. D. Sanchez-Yamagishi, K. Watanabe, T. Taniguchi, E. Kaxiras, R. C. Ashoori, and P. Jarillo-Herrero, Correlated insulator behaviour at half-filling in magic-angle graphene superlattices, Nature (London) **556**, 80 (2018).
[8] We additionally note an earlier experimental study on the electronic structure of moiré MoS_2/WSe_2 heterobilayers [142].
[9] Y. Choi, J. Kemmer, Y. Peng, A. Thomson, H. Arora, R. Polski, Y. Zhang, H. Ren, J. Alicea, G. Refael, F. von Oppen, K. Watanabe, T. Taniguchi, and S. Nadj-Perge, Electronic correlations in twisted bilayer graphene near the magic angle, Nat. Phys. **15**, 1174 (2019).
[10] Y. Jiang, X. Lai, K. Watanabe, T. Taniguchi, K. Haule, J. Mao, and E. Y. Andrei, Charge order and broken rotational symmetry in magic-angle twisted bilayer graphene, Nature (London) **573**, 91 (2019).
[11] A. Kerelsky, L. J. McGilly, D. M. Kennes, L. Xian, M. Yankowitz, S. Chen, K. Watanabe, T. Taniguchi, J. Hone, C. Dean, A. Rubio, and A. N. Pasupathy, Maximized electron interactions at the magic angle in twisted bilayer graphene, Nature (London) **572**, 95 (2019).
[12] Y. Cao, D. Rodan-Legrain, J. M. Park, F. N. Yuan, K. Watanabe, T. Taniguchi, R. M. Fernandes, L. Fu, and P. Jarillo-Herrero, Nematicity and competing orders in superconducting magic-angle graphene, Science **372**, 264 (2021).
[13] M. Yankowitz, S. Chen, H. Polshyn, Y. Zhang, K. Watanabe, T. Taniguchi, D. Graf, A. F. Young, and C. R. Dean, Tuning superconductivity in twisted bilayer graphene, Science **363**, 1059 (2019).
[14] H. Polshyn, M. Yankowitz, S. Chen, Y. Zhang, K. Watanabe, T. Taniguchi, C. R. Dean, and A. F. Young, Large linear-in-temperature resistivity in twisted bilayer graphene, Nat. Phys. **15**, 1011 (2019).
[15] Y. Cao, D. Chowdhury, D. Rodan-Legrain, O. Rubies-Bigorda, K. Watanabe, T. Taniguchi, T. Senthil, and P. Jarillo-Herrero, Strange Metal in Magic-Angle Graphene with near Planckian Dissipation, Phys. Rev. Lett. **124**, 076801 (2020).
[16] D. Wong, K. P. Nuckolls, M. Oh, B. Lian, Y. Xie, S. Jeon, K. Watanabe, T. Taniguchi, B. A. Bernevig, and A. Yazdani, Cascade of electronic transitions in magic-angle twisted bilayer graphene, Nature (London) **582**, 198 (2020).
[17] U. Zondiner, A. Rozen, D. Rodan-Legrain, Y. Cao, R. Queiroz, T. Taniguchi, K. Watanabe, Y. Oreg, F. von Oppen, A. Stern, E. Berg, P. Jarillo-Herrero, and S. Ilani, Cascade of phase transitions and Dirac revivals in magic-angle graphene, Nature (London) **582**, 203 (2020).
[18] X. Lu, P. Stepanov, W. Yang, M. Xie, M. A. Aamir, I. Das, C. Urgell, K. Watanabe, T. Taniguchi, G. Zhang, A. Bachtold, A. H. MacDonald, and D. K. Efetov, Superconductors, orbital magnets and correlated states in magic-angle bilayer graphene, Nature (London) **574**, 653 (2019).
[19] A. L. Sharpe, E. J. Fox, A. W. Barnard, J. Finney, K. Watanabe, T. Taniguchi, M. A. Kastner, and D. Goldhaber-Gordon, Evidence of orbital ferromagnetism in twisted bilayer graphene aligned to hexagonal boron nitride, Nano Lett. **21**, 4299 (2021).
[20] H. S. Arora, R. Polski, Y. Zhang, A. Thomson, Y. Choi, H. Kim, Z. Lin, I. Z. Wilson, X. Xu, J.-H. Chu, K. Watanabe, T. Taniguchi, J. Alicea, and S. Nadj-Perge, Superconductivity in metallic twisted bilayer graphene stabilized by WSe_2, Nature (London) **583**, 379 (2020).
[21] Y. Saito, J. Ge, K. Watanabe, T. Taniguchi, and A. F. Young, Independent superconductors and correlated insulators in twisted bilayer graphene, Nat. Phys. **16**, 926 (2020).
[22] P. Stepanov, I. Das, X. Lu, A. Fahimniya, K. Watanabe, T. Taniguchi, F. H. L. Koppens, J. Lischner, L. Levitov, and D. K. Efetov, Untying the insulating and superconducting orders in magic-angle graphene, Nature (London) **583**, 375 (2020).
[23] A. Uri, S. Grover, Y. Cao, J. A. Crosse, K. Bagani, D. Rodan-Legrain, Y. Myasoedov, K. Watanabe, T. Taniguchi, P. Moon, M. Koshino, P. Jarillo-Herrero, and E. Zeldov, Mapping the twist-angle disorder and Landau levels in magic-angle graphene, Nature (London) **581**, 47 (2020).
[24] Y. Saito, F. Yang, J. Ge, X. Liu, T. Taniguchi, K. Watanabe, J. I. A. Li, E. Berg, and A. F. Young, Isospin Pomeranchuk effect in twisted bilayer graphene, Nature (London) **592**, 220 (2021).
[25] A. Rozen, J. M. Park, U. Zondiner, Y. Cao, D. Rodan-Legrain, T. Taniguchi, K. Watanabe, Y. Oreg, A. Stern, E. Berg, P. Jarillo-Herrero, and S. Ilani, Entropic evidence for a Pomeranchuk effect in magic-angle graphene, Nature (London) **592**, 214 (2021).
[26] M. Oh, K. P. Nuckolls, D. Wong, R. L. Lee, X. Liu, K. Watanabe, T. Taniguchi, and A. Yazdani, Evidence for unconventional superconductivity in twisted bilayer graphene, Nature (London) **600**, 240 (2021).
[27] J.-X. Lin, Y.-H. Zhang, E. Morissette, Z. Wang, S. Liu, D. Rhodes, K. Watanabe, T. Taniguchi, J. Hone, and J. I. A. Li, Spin-orbit-driven ferromagnetism at half moiré filling in magic-angle twisted bilayer graphene, Science **375**, 437 (2022).
[28] A. L. Sharpe, E. J. Fox, A. W. Barnard, J. Finney, K. Watanabe, T. Taniguchi, M. A. Kastner, and D. Goldhaber-Gordon, Emergent ferromagnetism near three-quarters filling in twisted bilayer graphene, Science **365**, 605 (2019).
[29] M. Serlin, C. L. Tschirhart, H. Polshyn, Y. Zhang, J. Zhu, K. Watanabe, T. Taniguchi, L. Balents, and A. F. Young, Intrinsic quantized anomalous Hall effect in a moiré heterostructure, Science **367**, 900 (2020).

[30] K. P. Nuckolls, M. Oh, D. Wong, B. Lian, K. Watanabe, T. Taniguchi, B. A. Bernevig, and A. Yazdani, Strongly correlated Chern insulators in magic-angle twisted bilayer graphene, Nature (London) **588**, 610 (2020).

[31] Y. Choi, H. Kim, Y. Peng, A. Thomson, C. Lewandowski, R. Polski, Y. Zhang, H. S. Arora, K. Watanabe, T. Taniguchi, J. Alicea, and S. Nadj-Perge, Correlation-driven topological phases in magic-angle twisted bilayer graphene, Nature (London) **589**, 536 (2021).

[32] I. Das, X. Lu, J. Herzog-Arbeitman, Z.-D. Song, K. Watanabe, T. Taniguchi, B. A. Bernevig, and D. K. Efetov, Symmetry-broken Chern insulators and Rashba-like Landau-level crossings in magic-angle bilayer graphene, Nat. Phys. **17**, 710 (2021).

[33] Y. Saito, J. Ge, L. Rademaker, K. Watanabe, T. Taniguchi, D. A. Abanin, and A. F. Young, Hofstadter subband ferromagnetism and symmetry-broken Chern insulators in twisted bilayer graphene, Nat. Phys. **17**, 478 (2021).

[34] P. Stepanov, M. Xie, T. Taniguchi, K. Watanabe, X. Lu, A. H. MacDonald, B. A. Bernevig, and D. K. Efetov, Competing Zero-Field Chern Insulators in Superconducting Twisted Bilayer Graphene, Phys. Rev. Lett. **127**, 197701 (2021).

[35] J. M. Park, Y. Cao, K. Watanabe, T. Taniguchi, and P. Jarillo-Herrero, Flavour Hund's coupling, Chern gaps and charge diffusivity in moiré graphene, Nature (London) **592**, 43 (2021).

[36] C.-C. Tseng, X. Ma, Z. Liu, K. Watanabe, T. Taniguchi, J.-H. Chu, and M. Yankowitz, Anomalous Hall effect at half filling in twisted bilayer graphene, Nat. Phys. **18**, 1038 (2022).

[37] D. M. Kennes, J. Lischner, and C. Karrasch, Strong correlations and $d + id$ superconductivity in twisted bilayer graphene, Phys. Rev. B **98**, 241407(R) (2018).

[38] M. Koshino, N. F. Q. Yuan, T. Koretsune, M. Ochi, K. Kuroki, and L. Fu, Maximally Localized Wannier Orbitals and the Extended Hubbard Model for Twisted Bilayer Graphene, Phys. Rev. X **8**, 031087 (2018).

[39] H. C. Po, L. Zou, A. Vishwanath, and T. Senthil, Origin of Mott Insulating Behavior and Superconductivity in Twisted Bilayer Graphene, Phys. Rev. X **8**, 031089 (2018).

[40] F. Wu, A. H. MacDonald, and I. Martin, Theory of Phonon-Mediated Superconductivity in Twisted Bilayer Graphene, Phys. Rev. Lett. **121**, 257001 (2018).

[41] J. Kang and O. Vafek, Strong Coupling Phases of Partially Filled Twisted Bilayer Graphene Narrow Bands, Phys. Rev. Lett. **122**, 246401 (2019).

[42] B. Lian, Z. Wang, and B. A. Bernevig, Twisted Bilayer Graphene: A Phonon-Driven Superconductor, Phys. Rev. Lett. **122**, 257002 (2019).

[43] K. Seo, V. N. Kotov, and B. Uchoa, Ferromagnetic Mott State in Twisted Graphene Bilayers at the Magic Angle, Phys. Rev. Lett. **122**, 246402 (2019).

[44] N. Bultinck, S. Chatterjee, and M. P. Zaletel, Mechanism for Anomalous Hall Ferromagnetism in Twisted Bilayer Graphene, Phys. Rev. Lett. **124**, 166601 (2020).

[45] N. Bultinck, E. Khalaf, S. Liu, S. Chatterjee, A. Vishwanath, and M. P. Zaletel, Ground State and Hidden Symmetry of Magic-Angle Graphene at Even Integer Filling, Phys. Rev. X **10**, 031034 (2020).

[46] M. Christos, S. Sachdev, and M. S. Scheurer, Superconductivity, correlated insulators, and Wess-Zumino-Witten terms in twisted bilayer graphene, Proc. Natl. Acad. Sci. USA **117**, 29543 (2020).

[47] M. Xie and A. H. MacDonald, Nature of the Correlated Insulator States in Twisted Bilayer Graphene, Phys. Rev. Lett. **124**, 097601 (2020).

[48] K. Hejazi, X. Chen, and L. Balents, Hybrid Wannier Chern bands in magic angle twisted bilayer graphene and the quantized anomalous Hall effect, Phys. Rev. Res. **3**, 013242 (2021).

[49] E. Khalaf, S. Chatterjee, N. Bultinck, M. P. Zaletel, and A. Vishwanath, Charged skyrmions and topological origin of superconductivity in magic-angle graphene, Sci. Adv. **7**, eabf5299 (2021).

[50] S. Liu, E. Khalaf, J. Y. Lee, and A. Vishwanath, Nematic topological semimetal and insulator in magic-angle bilayer graphene at charge neutrality, Phys. Rev. Res. **3**, 013033 (2021).

[51] D. E. Parker, T. Soejima, J. Hauschild, M. P. Zaletel, and N. Bultinck, Strain-Induced Quantum Phase Transitions in Magic-Angle Graphene, Phys. Rev. Lett. **127**, 027601 (2021).

[52] G. Shavit, E. Berg, A. Stern, and Y. Oreg, Theory of Correlated Insulators and Superconductivity in Twisted Bilayer Graphene, Phys. Rev. Lett. **127**, 247703 (2021).

[53] G. Wagner, Y. H. Kwan, N. Bultinck, S. H. Simon, and S. A. Parameswaran, Global Phase Diagram of the Normal State of Twisted Bilayer Graphene, Phys. Rev. Lett. **128**, 156401 (2022).

[54] G. W. Burg, J. Zhu, T. Taniguchi, K. Watanabe, A. H. MacDonald, and E. Tutuc, Correlated Insulating States in Twisted Double Bilayer Graphene, Phys. Rev. Lett. **123**, 197702 (2019).

[55] G. Chen, A. L. Sharpe, P. Gallagher, I. T. Rosen, E. J. Fox, L. Jiang, B. Lyu, H. Li, K. Watanabe, T. Taniguchi, J. Jung, Z. Shi, D. Goldhaber-Gordon, Y. Zhang, and F. Wang, Signatures of tunable superconductivity in a trilayer graphene moiré superlattice, Nature (London) **572**, 215 (2019).

[56] G. Chen, L. Jiang, S. Wu, B. Lyu, H. Li, B. L. Chittari, K. Watanabe, T. Taniguchi, Z. Shi, J. Jung, Y. Zhang, and F. Wang, Evidence of a gate-tunable Mott insulator in a trilayer graphene moiré superlattice, Nat. Phys. **15**, 237 (2019).

[57] Y. Cao, D. Rodan-Legrain, O. Rubies-Bigorda, J. M. Park, K. Watanabe, T. Taniguchi, and P. Jarillo-Herrero, Tunable correlated states and spin-polarized phases in twisted bilayer-bilayer graphene, Nature (London) **583**, 215 (2020).

[58] Y. Cao, J. M. Park, K. Watanabe, T. Taniguchi, and P. Jarillo-Herrero, Pauli-limit violation and re-entrant superconductivity in moiré graphene, Nature (London) **595**, 526 (2021).

[59] X. Liu, Z. Hao, E. Khalaf, J. Y. Lee, Y. Ronen, H. Yoo, D. H. Najafabadi, K. Watanabe, T. Taniguchi, A. Vishwanath, and P. Kim, Tunable spin-polarized correlated states in twisted double bilayer graphene, Nature (London) **583**, 221 (2020).

[60] C. Shen, Y. Chu, Q. Wu, N. Li, S. Wang, Y. Zhao, J. Tang, J. Liu, J. Tian, K. Watanabe, T. Taniguchi, R. Yang, Z. Y. Meng, D. Shi, O. V. Yazyev, and G. Zhang, Correlated states in twisted double bilayer graphene, Nat. Phys. **16**, 520 (2020).

[61] Z. Hao, A. M. Zimmerman, P. Ledwith, E. Khalaf, D. H. Najafabadi, K. Watanabe, T. Taniguchi, A. Vishwanath, and P. Kim, Electric field–tunable superconductivity in alternating-twist magic-angle trilayer graphene, Science **371**, 1133 (2021).

[62] X. Liu, Z. Wang, K. Watanabe, T. Taniguchi, O. Vafek, and J. I. A. Li, Tuning electron correlation in magic-angle twisted bilayer graphene using Coulomb screening, Science **371**, 1261 (2021).

[63] J. M. Park, Y. Cao, K. Watanabe, T. Taniguchi, and P. Jarillo-Herrero, Tunable strongly coupled superconductivity in magic-angle twisted trilayer graphene, Nature (London) **590**, 249 (2021).

[64] E. C. Regan, D. Wang, C. Jin, M. I. B. Utama, B. Gao, X. Wei, S. Zhao, W. Zhao, Z. Zhang, K. Yumigeta, M. Blei, J. D. Carlström, K. Watanabe, T. Taniguchi, S. Tongay, M. Crommie, A. Zettl, and F. Wang, Mott and generalized Wigner crystal states in WSe_2/WS_2 moiré superlattices, Nature (London) **579**, 359 (2020).

[65] Y. Shimazaki, I. Schwartz, K. Watanabe, T. Taniguchi, M. Kroner, and A. Imamoğlu, Strongly correlated electrons and hybrid excitons in a moiré heterostructure, Nature (London) **580**, 472 (2020).

[66] Y. Tang, L. Li, T. Li, Y. Xu, S. Liu, K. Barmak, K. Watanabe, T. Taniguchi, A. H. MacDonald, J. Shan, and K. F. Mak, Simulation of Hubbard model physics in WSe_2/WS_2 moiré superlattices. Nature (London) **579**, 353 (2020).

[67] L. Wang, E.-M. Shih, A. Ghiotto, L. Xian, D. A. Rhodes, C. Tan, M. Claassen, D. M. Kennes, Y. Bai, B. Kim, K. Watanabe, T. Taniguchi, X. Zhu, J. Hone, A. Rubio, A. N. Pasupathy, and C. R. Dean, Correlated electronic phases in twisted bilayer transition metal dichalcogenides, Nat. Mater. **19**, 861 (2020).

[68] Y. Xu, S. Liu, D. A. Rhodes, K. Watanabe, T. Taniguchi, J. Hone, V. Elser, K. F. Mak, and J. Shan, Correlated insulating states at fractional fillings of moiré superlattices, Nature (London) **587**, 214 (2020).

[69] Z. Zhang, Y. Wang, K. Watanabe, T. Taniguchi, K. Ueno, E. Tutuc, and B. J. LeRoy, Flat bands in twisted bilayer transition metal dichalcogenides, Nat. Phys. **16**, 1093 (2020).

[70] S. Tomonaga, Remarks on Bloch's method of sound waves applied to many-fermion problems, Prog. Theor. Phys. **5**, 544 (1950).

[71] J. M. Luttinger, An exactly soluble model of a many-fermion system, J. Math. Phys. **4**, 1154 (1963).

[72] F. D. M. Haldane, Luttinger liquid theory of one-dimensional quantum fluids. I. Properties of the Luttinger model and their extension to the general 1D interacting spinless Fermi gas, J. Phys. C: Solid State Phys. **14**, 2585 (1981).

[73] P. San-Jose and E. Prada, Helical networks in twisted bilayer graphene under interlayer bias, Phys. Rev. B **88**, 121408(R) (2013).

[74] N. N. T. Nam and M. Koshino, Lattice relaxation and energy band modulation in twisted bilayer graphene, Phys. Rev. B **96**, 075311 (2017).

[75] D. K. Efimkin and A. H. MacDonald, Helical network model for twisted bilayer graphene, Phys. Rev. B **98**, 035404 (2018).

[76] S. Huang, K. Kim, D. K. Efimkin, T. Lovorn, T. Taniguchi, K. Watanabe, A. H. MacDonald, E. Tutuc, and B. J. LeRoy, Topologically Protected Helical States in Minimally Twisted Bilayer Graphene, Phys. Rev. Lett. **121**, 037702 (2018).

[77] Y. Xie, B. Lian, B. Jäck, X. Liu, C.-L. Chiu, K. Watanabe, T. Taniguchi, B. A. Bernevig, and A. Yazdani, Spectroscopic signatures of many-body correlations in magic-angle twisted bilayer graphene, Nature (London) **572**, 101 (2019).

[78] P. Rickhaus, J. Wallbank, S. Slizovskiy, R. Pisoni, H. Overweg, Y. Lee, M. Eich, M.-H. Liu, K. Watanabe, T. Taniguchi, T. Ihn, and K. Ensslin, Transport through a network of topological channels in twisted bilayer graphene, Nano Lett. **18**, 6725 (2018).

[79] The STM experiments revealed additional features around AA-stacking regions, which inspired Refs. [143–145] to construct a heavy-fermion model.

[80] X.-C. Wu, C.-M. Jian, and C. Xu, Coupled-wire description of the correlated physics in twisted bilayer graphene, Phys. Rev. B **99**, 161405(R) (2019).

[81] Y.-Z. Chou, Y.-P. Lin, S. Das Sarma, and R. M. Nandkishore, Superconductor versus insulator in twisted bilayer graphene, Phys. Rev. B **100**, 115128 (2019).

[82] C. Chen, A. H. Castro Neto, and V. M. Pereira, Correlated states of a triangular net of coupled quantum wires: Implications for the phase diagram of marginally twisted bilayer graphene, Phys. Rev. B **101**, 165431 (2020).

[83] Y.-Z. Chou, F. Wu, and J. D. Sau, Charge density wave and finite-temperature transport in minimally twisted bilayer graphene, Phys. Rev. B **104**, 045146 (2021).

[84] J. M. Lee, M. Oshikawa, and G. Y. Cho, Non-Fermi Liquids in Conducting Two-Dimensional Networks, Phys. Rev. Lett. **126**, 186601 (2021).

[85] V. J. Emery, E. Fradkin, S. A. Kivelson, and T. C. Lubensky, Quantum Theory of the Smectic Metal State in Stripe Phases, Phys. Rev. Lett. **85**, 2160 (2000).

[86] A. Vishwanath and D. Carpentier, Two-Dimensional Anisotropic Non-Fermi-Liquid Phase of Coupled Luttinger Liquids, Phys. Rev. Lett. **86**, 676 (2001).

[87] R. Mukhopadhyay, C. L. Kane, and T. C. Lubensky, Crossed sliding Luttinger liquid phase, Phys. Rev. B **63**, 081103(R) (2001).

[88] R. Mukhopadhyay, C. L. Kane, and T. C. Lubensky, Sliding Luttinger liquid phases, Phys. Rev. B **64**, 045120 (2001).

[89] C. L. Kane, R. Mukhopadhyay, and T. C. Lubensky, Fractional Quantum Hall Effect in an Array of Quantum Wires, Phys. Rev. Lett. **88**, 036401 (2002).

[90] J. Klinovaja and D. Loss, Topological Edge States and Fractional Quantum Hall Effect from Umklapp Scattering, Phys. Rev. Lett. **111**, 196401 (2013).

[91] J. Klinovaja and Y. Tserkovnyak, Quantum spin Hall effect in strip of stripes model, Phys. Rev. B **90**, 115426 (2014).

[92] J. Klinovaja and D. Loss, Integer and fractional quantum Hall effect in a strip of stripes, Eur. Phys. J. B **87**, 171 (2014).

[93] T. Neupert, C. Chamon, C. Mudry, and R. Thomale, Wire deconstructionism of two-dimensional topological phases, Phys. Rev. B **90**, 205101 (2014).

[94] E. Sagi and Y. Oreg, Non-Abelian topological insulators from an array of quantum wires, Phys. Rev. B **90**, 201102(R) (2014).

[95] J. C. Y. Teo and C. L. Kane, From Luttinger liquid to non-Abelian quantum Hall states, Phys. Rev. B **89**, 085101 (2014).

[96] J. Klinovaja, Y. Tserkovnyak, and D. Loss, Integer and fractional quantum anomalous Hall effect in a strip of stripes model, Phys. Rev. B **91**, 085426 (2015).

[97] R. A. Santos, C.-W. Huang, Y. Gefen, and D. B. Gutman, Fractional topological insulators: From sliding Luttinger liquids to Chern-Simons theory, Phys. Rev. B **91**, 205141 (2015).

[98] Y. Imamura, K. Totsuka, and T. H. Hansson, From coupled-wire construction of quantum Hall states to wave functions and hydrodynamics, Phys. Rev. B **100**, 125148 (2019).
[99] T. Meng, Coupled-wire constructions: A Luttinger liquid approach to topology, Eur. Phys. J. Spec. Top. **229**, 527 (2020).
[100] P. Wang, G. Yu, Y. H. Kwan, Y. Jia, S. Lei, S. Klemenz, F. A. Cevallos, R. Singha, T. Devakul, K. Watanabe, T. Taniguchi, S. L. Sondhi, R. J. Cava, L. M. Schoop, S. A. Parameswaran, and S. Wu, One-dimensional Luttinger liquids in a two-dimensional moiré lattice, Nature (London) **605**, 57 (2022).
[101] M. Fujimoto, T. Kawakami, and M. Koshino, Perfect one-dimensional interface states in a twisted stack of three-dimensional topological insulators, Phys. Rev. Res. **4**, 043209 (2022).
[102] I. Tateishi and M. Hirayama, Quantum spin Hall effect from multiscale band inversion in twisted bilayer $Bi_2(Te_{1-x}Se_x)_3$, Phys. Rev. Res. **4**, 043045 (2022).
[103] C.-C. Hsu, M. L. Teague, J.-Q. Wang, and N.-C. Yeh, Nanoscale strain engineering of giant pseudo-magnetic fields, valley polarization, and topological channels in graphene, Sci. Adv. **6**, eaat9488 (2020).
[104] T. Giamarchi, *Quantum Physics in One Dimension* (Oxford University Press, New York, 2003).
[105] See Supplemental Material at http://link.aps.org/supplemental/10.1103/PhysRevB.108.L121409 for technical details, which includes Refs. [146–148].
[106] G. Shavit and Y. Oreg, Fractional Conductance in Strongly Interacting 1D Systems, Phys. Rev. Lett. **123**, 036803 (2019).
[107] C.-H. Hsu, F. Ronetti, P. Stano, J. Klinovaja, and D. Loss, Universal conductance dips and fractional excitations in a two-subband quantum wire, Phys. Rev. Res. **2**, 043208 (2020).
[108] T. Giamarchi, Umklapp process and resistivity in one-dimensional fermion systems, Phys. Rev. B **44**, 2905 (1991).
[109] R. Landauer, Spatial variation of currents and fields due to localized scatterers in metallic conduction, IBM J. Res. Dev. **1**, 223 (1957).
[110] R. Landauer, Electrical resistance of disordered one-dimensional lattices, Philos. Mag. **21**, 863 (1970).
[111] M. Büttiker, Absence of backscattering in the quantum Hall effect in multiprobe conductors, Phys. Rev. B **38**, 9375 (1988).
[112] S. Datta, *Electronic Transport in Mesoscopic Systems* (Cambridge University Press, Cambridge, 1995).
[113] M. Bockrath, D. H. Cobden, J. Lu, A. G. Rinzler, R. E. Smalley, L. Balents, and P. L. McEuen, Luttinger-liquid behaviour in carbon nanotubes, Nature (London) **397**, 598 (1999).
[114] L. Balents, Orthogonality catastrophes in carbon nanotubes, arXiv:cond-mat/9906032.
[115] R. Stühler, F. Reis, T. Müller, T. Helbig, T. Schwemmer, R. Thomale, J. Schäfer, and R. Claessen, Tomonaga-Luttinger liquid in the edge channels of a quantum spin Hall insulator, Nat. Phys. **16**, 47 (2020).
[116] C.-H. Hsu, P. Stano, J. Klinovaja, and D. Loss, Helical liquids in semiconductors, Semicond. Sci. Technol. **36**, 123003 (2021).
[117] C. L. Kane, M. P. A. Fisher, and J. Polchinski, Randomness at the Edge: Theory of Quantum Hall Transport at Filling $\nu = 2/3$, Phys. Rev. Lett. **72**, 4129 (1994).
[118] C. L. Kane and M. P. A. Fisher, Impurity scattering and transport of fractional quantum Hall edge states, Phys. Rev. B **51**, 13449 (1995).
[119] C. L. Kane and M. P. A. Fisher, Edge-state transport, in *Perspectives in Quantum Hall Effects*, edited by S. D. Sarma and A. Pinczuk (John Wiley & Sons, 1996), pp. 109–159.
[120] M. P. A. Fisher and L. I. Glazman, Transport in a one-dimensional luttinger liquid, in *Mesoscopic Electron Transport*, edited by L. L. Sohn, L. P. Kouwenhoven, and G. Schön (Springer, Netherlands, 1997), pp. 331–373.
[121] A. M. Chang, Chiral Luttinger liquids at the fractional quantum Hall edge, Rev. Mod. Phys. **75**, 1449 (2003).
[122] C.-H. Hsu, P. Stano, Y. Sato, S. Matsuo, S. Tarucha, and D. Loss, Charge transport of a spin-orbit-coupled Luttinger liquid, Phys. Rev. B **100**, 195423 (2019).
[123] C. L. Kane and M. P. A. Fisher, Nonequilibrium Noise and Fractional Charge in the Quantum Hall Effect, Phys. Rev. Lett. **72**, 724 (1994).
[124] L. Saminadayar, D. C. Glattli, Y. Jin, and B. Etienne, Observation of the $e/3$ Fractionally Charged Laughlin Quasiparticle, Phys. Rev. Lett. **79**, 2526 (1997).
[125] R. de-Picciotto, M. Reznikov, M. Heiblum, V. Umansky, G. Bunin, and D. Mahalu, Direct observation of a fractional charge, Nature (London) **389**, 162 (1997).
[126] C. R. Dean, L. Wang, P. Maher, C. Forsythe, F. Ghahari, Y. Gao, J. Katoch, M. Ishigami, P. Moon, M. Koshino, T. Taniguchi, K. Watanabe, K. L. Shepard, J. Hone, and P. Kim, Hofstadter's butterfly and the fractal quantum Hall effect in moiré superlattices, Nature (London) **497**, 598 (2013).
[127] B. Hunt, J. D. Sanchez-Yamagishi, A. F. Young, M. Yankowitz, B. J. LeRoy, K. Watanabe, T. Taniguchi, P. Moon, M. Koshino, P. Jarillo-Herrero, and R. C. Ashoori, Massive Dirac fermions and Hofstadter butterfly in a van der Waals heterostructure, Science **340**, 1427 (2013).
[128] L. A. Ponomarenko, R. V. Gorbachev, G. L. Yu, D. C. Elias, R. Jalil, A. A. Patel, A. Mishchenko, A. S. Mayorov, C. R. Woods, J. R. Wallbank, M. Mucha-Kruczynski, B. A. Piot, M. Potemski, I. V. Grigorieva, K. S. Novoselov, F. Guinea, V. I. Fal'ko, and A. K. Geim, Cloning of Dirac fermions in graphene superlattices, Nature (London) **497**, 594 (2013).
[129] P. Moon and M. Koshino, Electronic properties of graphene/hexagonal-boron-nitride moiré superlattice, Phys. Rev. B **90**, 155406 (2014).
[130] H. Kim, N. Leconte, B. L. Chittari, K. Watanabe, T. Taniguchi, A. H. MacDonald, J. Jung, and S. Jung, Accurate gap determination in monolayer and bilayer graphene/h-BN moiré superlattices, Nano Lett. **18**, 7732 (2018).
[131] M. Kindermann, B. Uchoa, and D. L. Miller, Zero-energy modes and gate-tunable gap in graphene on hexagonal boron nitride, Phys. Rev. B **86**, 115415 (2012).
[132] P. Fendley, Parafermionic edge zero modes in Z_n-invariant spin chains, J. Stat. Mech. (2012) P11020.
[133] D. J. Clarke, J. Alicea, and K. Shtengel, Exotic non-Abelian anyons from conventional fractional quantum Hall states, Nat. Commun. **4**, 1348 (2013).
[134] J. Klinovaja, A. Yacoby, and D. Loss, Kramers pairs of Majorana fermions and parafermions in fractional topological insulators, Phys. Rev. B **90**, 155447 (2014).
[135] R. S. K. Mong, D. J. Clarke, J. Alicea, N. H. Lindner, P. Fendley, C. Nayak, Y. Oreg, A. Stern, E. Berg, K.

Shtengel, and M. P. A. Fisher, Universal Topological Quantum Computation from a Superconductor-Abelian Quantum Hall Heterostructure, Phys. Rev. X **4**, 011036 (2014).

[136] T. Meng and E. Sela, Time reversal symmetry broken fractional topological phases at zero magnetic field, Phys. Rev. B **90**, 235425 (2014).

[137] Y. Oreg, E. Sela, and A. Stern, Fractional helical liquids in quantum wires, Phys. Rev. B **89**, 115402 (2014).

[138] E. Sagi, Y. Oreg, A. Stern, and B. I. Halperin, Imprint of topological degeneracy in quasi-one-dimensional fractional quantum Hall states, Phys. Rev. B **91**, 245144 (2015).

[139] E. Sagi, A. Haim, E. Berg, F. von Oppen, and Y. Oreg, Fractional chiral superconductors, Phys. Rev. B **96**, 235144 (2017).

[140] K. Laubscher, D. Loss, and J. Klinovaja, Fractional topological superconductivity and parafermion corner states, Phys. Rev. Res. **1**, 032017(R) (2019).

[141] K. Laubscher, D. Loss, and J. Klinovaja, Majorana and parafermion corner states from two coupled sheets of bilayer graphene, Phys. Rev. Res. **2**, 013330 (2020).

[142] C. Zhang, C.-P. Chuu, X. Ren, M.-Y. Li, L.-J. Li, C. Jin, M.-Y. Chou, and C.-K. Shih, Interlayer couplings, moiré patterns, and 2D electronic superlattices in MoS_2/WSe_2 hetero-bilayers, Sci. Adv. **3**, e1601459 (2017).

[143] Z.-D. Song and B. A. Bernevig, Magic-Angle Twisted Bilayer Graphene as a Topological Heavy Fermion Problem, Phys. Rev. Lett. **129**, 047601 (2022).

[144] H. Shi and X. Dai, Heavy-fermion representation for twisted bilayer graphene systems, Phys. Rev. B **106**, 245129 (2022).

[145] L. L. H. Lau and P. Coleman, Topological mixed valence model for twisted bilayer graphene, arXiv:2303.02670.

[146] P. Lecheminant, A. O. Gogolin, and A. A. Nersesyan, Criticality in self-dual sine-Gordon models, Nucl. Phys. B **639**, 502 (2002).

[147] F. Ronetti, D. Loss, and J. Klinovaja, Clock model and parafermions in Rashba nanowires, Phys. Rev. B **103**, 235410 (2021).

[148] T. Meng, P. Stano, J. Klinovaja, and D. Loss, Helical nuclear spin order in a strip of stripes in the quantum Hall regime, Eur. Phys. J. B **87**, 203 (2014).